

Chapter 5: Energy Decay in Isotropic Turbulence

Part 2: Modes of Isotropic Decay and Self-Similarity

Additional assumptions are required to close the equations derived for the decay of isotropic turbulence. The interest is in the decay at both the low and high turbulent Reynolds number $R_T = \frac{k^2}{\nu \varepsilon} = \frac{\sqrt{k} k^{3/2} / \varepsilon}{\nu}$ limits. Several theories, but all result in a power law in time for the decay process, i.e.,

$$k \sim (t - t_0)^{-n}$$

where t_0 represents a virtual time origin.

One approach is to assume full or partial similarity as the flow evolves. For very **low R_T** assuming full similarity (final period of decay), vortex stretching can be neglected and the solution to the simplified k, ε equations along with the solution of the Karman-Howarth equation for $f(r, t)$ shows that k follows a **$t^{-5/2}$** power law. Whereas for High R_T , vortex stretching cannot be neglected and n and other statistical quantities depend on different theories. For full similarity and **high R_T** , $k \sim t^{-1}$. One alternative, for example, is Saffman theory, which predicts $k \sim t^{-6/5}$, which resembles the higher Re experimental data.

Validation requires data for $-n$ and other flow statistics; however, many difficulties obtaining archival EFD and DNS for homogeneous isotropic turbulence: finite domain, anisotropy, and initial conditions.

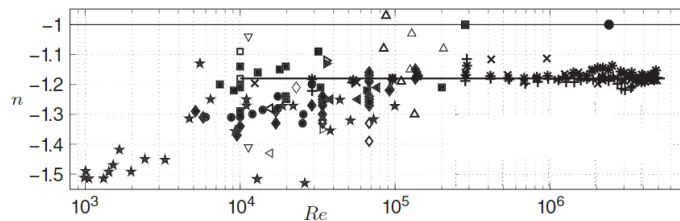


Figure 5.6 Measured power law exponents in decaying homogeneous turbulence from numerous experiments [9]. Filled symbols represent traditional turbulence behind a grid of bars. Open symbols are other turbulence sources. The symbols with \times , $*$, and $+$ are from three different probes used in decaying turbulence behind a grid of bars for which the Reynolds number was changed only by altering the viscosity of the working fluid. Used by permission of AIP.

The following provides an overview of full/complete similarity results for fixed point/equilibrium states for low and high Re initial conditions. Part 3 shows results for more advanced approaches.

Since isotropic decay assumes homogeneous conditions over all space, there is no externally imposed geometric length scale. For self-similarity $L = L(t)$ such that multi-point velocity correlation functions retain the same form independent of time.

While there is no externally imposed length scale on the isotropic decay process; nonetheless; the turbulence has two intrinsic length scales associated with the isotropic motion, i.e., (1) scales in the dissipation range depending on viscosity and (2) integral length scales of the turbulence associated with the larger energy containing eddies. The presence of two length scales causes difficulties in obtaining similarity solutions. Early research used the Taylor integral length scale Λ in seeking self-similarity, but later greater success was found using the Taylor micro scale λ .

The Taylor micro scale is the only similarity length scale that can yield complete self-preserving solutions to the full viscous equations of motion for isotropic turbulence. For similarity:

$$f(r, t) = \tilde{f}\left(\frac{r}{L(t)} = \eta\right) = \frac{\overline{u(x, t)u(x + r, t)}}{\overline{u^2}} \quad (1a)$$

$$k(r, t) = \tilde{k}\left(\frac{r}{L(t)} = \eta\right) = \frac{\overline{u(x, t)u(x, t)u(x + r, t)}}{u_{rms}^3} \quad (1b)$$

Where $\eta = r/L(t)$ is the similarity variable. The turbulent decay exhibits complete self-similarity, i.e., self-preserving if scaling holds for all r or partial/incomplete if only holds for limited range of r or for limited ranges of R_λ .

Under the assumption of complete similarity, the decay becomes solvable albeit with some unresolved issues especially regarding the entire decay process.

Recall definitions from Chapters 2 and 4 Part 3

$$\lambda_f = \sqrt{2}\lambda_g \quad (2)$$

$$\lambda_f^2 = -2/f''(0)$$

Therefore ($f' = \tilde{f}'/L; f'' = \tilde{f}''/L^2$):

$$\lambda_f^2/L^2 = -2/\tilde{f}''(0)$$

Where $\tilde{f}''(0) \neq f(t)$ according to Eq. (1a), i.e., $\tilde{f}\left(\frac{r}{L(t)} = 0\right)$ and $\tilde{k}\left(\frac{r}{L(t)} = 0\right)$ are not a function of time. Thus,

$$\lambda_f^2 \propto L^2$$

and can assume $L = \lambda_g$, using Eq. (2). Similarly, using the relation

$$k'''(0) = -S_k \left(\frac{\varepsilon}{15\overline{u^2\nu}} \right)^{3/2}$$

Substituting $\varepsilon = \frac{15\overline{u^2\nu}}{\lambda_g^2}$ and assuming self-similarity ($k' = \frac{\tilde{k}'}{L}; k'' = \frac{\tilde{k}''}{L^2}; k''' = \frac{\tilde{k}'''}{L^3}$) yields

$$\frac{\tilde{k}'''(0)}{\lambda_g^3} = -S_k \left(\frac{15\overline{u^2\nu}}{15\overline{u^2\nu}} \frac{1}{\lambda_g^2} \right)^{3/2} = -\frac{S_k}{\lambda_g^3}$$

$$-S_k = \tilde{k}'''(0)$$

$$S_K^* = \frac{7}{3\sqrt{15}} S_k$$

Similarly, starting from [Part 1 Eq. (18)]

$$f^{IV}(0) = G \left(\frac{\varepsilon}{15\overline{u^2\nu}} \right)^2$$

The following relation is obtained,

$$\frac{\tilde{f}^{IV}(0)}{\lambda_g^4} = G \left(\frac{15\overline{u^2\nu}}{15\overline{u^2\nu}\lambda_g^2} \frac{1}{\lambda_g^2} \right)^2 = \frac{G}{\lambda_g^4}$$

$$G = \tilde{f}^{IV}(0)$$

$$G^* = \frac{7}{15} G$$

i.e., S_k and G are constant during self-similar decay. This is a direct consequence of the self-similarity hypothesis, and it is the reason why the GDE represent a closed system of equations, under self-similarity:

$$\frac{dk}{dt} = -\varepsilon \quad (3a)$$

$$\frac{d\varepsilon}{dt} = S_{k_0}^* R_T^{1/2} \frac{\varepsilon^2}{k} - G_0^* \frac{\varepsilon^2}{k} \quad (3b)$$

where $S_{k_0}^*$ and G_0^* are constants provided by assigned values based on experiments or DNS. Alternatively, can solve single equation for $R_T^*(\tau) = R_T(t) = k^2(t)/\nu\varepsilon(t)$

$$\frac{dR_T^*}{d\tau} = R_T^* (G_0^* - 2 - S_{k_0}^* \sqrt{R_T^*}) \quad (4)$$

From an initial state with $R_T^*(0) \gg 1$ to a time when $R_T^* \ll 1$.

Part 3 uses assigned values of $S_{k_0}^*$ and G_0^* to solve the K-H equations for \tilde{f} and \tilde{k} for the final decay, which are used below to confirm the assigned values showing that assigning either $S_{k_0}^*$ and G_0^* or \tilde{f} and \tilde{k} are equivalent.

Fixed Point Analysis

Consider solutions for $\frac{dR_T^*}{d\tau} = 0$, i.e., $R_T^* = \text{constant}$, which are “attracting” solutions in dynamical sense such that the IC $R_{T_0}^*$ converges towards $R_{T_\infty}^*$ solutions as $t \rightarrow \infty$.

Dynamical system theory indicates that even for G^* and S_k^* functions of time, fixed point solutions are stable nodes, which implies that the solutions of the k and ε equations are unaffected by small changes in G^* and S_k^* during the isotropic decay.

Fixed points $R_{T_\infty}^*$ are solutions of

$$R_{T_\infty}^* \left(G_0^* - 2 - S_{k_0}^* \sqrt{R_{T_\infty}^*} \right) = 0 \quad (5)$$

which is satisfied by either,

$$R_{T_\infty}^* = 0 \quad (6)$$

or

$$R_{T_\infty}^* = \left(\frac{G_0^* - 2}{S_{k_0}^*} \right)^2 \quad (7)$$

Solutions beginning with IC $R_T^*(0)$ will move toward one or the other depending on the value of G_0^* . Eq. (6) is reached for all IC if $G_0^* \leq 2$. Whereas Eq. (7) is reached for all IC if $G_0^* > 2$. These behaviors are evident from examination Eq. (4).

For $G_0^* < 2$ term in (...) on RHS of Eq. (4) is not zero and always negative such that R_T^* must decay to zero.

For $G_0^* > 2$ the RHS is positive for $R_{T_0}^* < R_{T_\infty}^*$ and negative for $R_{T_0}^* > R_{T_\infty}^*$. In either case the RHS will raise or lower R_T^* until it converges to $R_{T_\infty}^*$, which in this case $R_{T_\infty}^* \neq 0$.

The two fixed-point solutions represent different equilibrium states of isotropic turbulence decay.

Note that:

(1) $G_0^* \leq 2$ solutions require small R_{T_0} since as will be shown for large R_{T_0} , $\frac{dR_T^*}{d\tau} \neq 0$ and solutions Eq. (4) lead to unphysical behavior.

(2) For $G_0^* > 2$ the decay process cannot achieve $R_{T_\infty}^* = 0$; therefore, it is implied that self-similarity throughout the entire decay process is not feasible, which is likely due to using $L = \lambda$, since λ cannot characterize turbulence at larger scales, where anisotropy is important and Λ is more relevant.

(3) That even though $R_{T_\infty}^* = \frac{k_\infty^2}{\nu \varepsilon_\infty} = \text{constant}$, i.e., not $f(t)$ during fixed point analysis, k and ε are $f(t)$ but must decay such that $R_T^* = \text{constant}$.

Final Period of Isotropic Decay

Fixed point (equilibrium solution) $R_{T_\infty}^* = 0$ is the end point of the decay process, in which there is no motion. Near this end point $R_{T_0} = k_0^2/\nu\varepsilon_0 \ll 1$, but $\neq 0$ and it is of interest to examine the properties of turbulence in this weakened condition.

Rewriting Eq. (3) $\left(\frac{d\varepsilon}{dt} = S_{k_0}^* R_T^{\frac{1}{2}} \frac{\varepsilon^2}{k} - G_0^* \frac{\varepsilon^2}{k}\right)$ in the form,

$$\frac{d\varepsilon}{dt} = \left(\frac{S_{k_0}^* R_T^{1/2}}{G_0^*} - 1 \right) G_0^* \frac{\varepsilon^2}{k} \quad (8)$$

For

$$\frac{S_{k_0}^* R_T^{1/2}}{G_0^*} \ll 1 \quad (9)$$

vortex stretching is negligible. Recall:

$$Re_T = \frac{k^2}{\nu \varepsilon} = \frac{3}{20} R_\lambda^2 \quad \left(R_\lambda = \frac{\lambda_g u_{rms}}{\nu} \right)$$

Low R_λ experiments measured $S_k \approx 0.5$ and $G \approx 3$, so that $S_{k_0}^* \approx 0.3$ and $G_0^* \approx 1.4 < 2$. Using these values in Eq. (9) yields,

$$\frac{0.3 \times R_T^{\frac{1}{2}}}{1.4} = 0.21\sqrt{R_T} = 0.21 \times 0.32 = 0.07 \quad \text{for } R_T = 0.1$$

Note that the above estimates for $S_{k_0}^*$ and G_0^* are only used to confirm Eq. (9), i.e., the vortex stretching term can be neglected.

Therefore, for $R_{T_0} < 0.1$, i.e., in the vicinity of $R_{T_\infty} = 0$, the coupled equations for k and ε reduce to

$$\frac{dk}{dt} = -\varepsilon \quad (10)$$

$$\frac{d\varepsilon}{dt} = -G_0^* \frac{\varepsilon^2}{k} \quad (11)$$

Assuming power laws for k and ε , these have the exact solutions,

$$\begin{aligned} \frac{k}{k_0} &= \left(1 + \frac{t}{\alpha T_{t_0}}\right)^{-\alpha} \\ \frac{\varepsilon}{\varepsilon_0} &= \left(1 + \frac{t}{\alpha T_{t_0}}\right)^{-1-\alpha} \\ \alpha &= \frac{1}{G_0^* - 1} = f(G_0^*) \quad (12) \end{aligned}$$

and k_0, ε_0 and $T_{t_0} = k_0/\varepsilon_0$ are the initial values of the flow properties, i.e., IC. After t advances several multiples of T_{t_0} , such that $t/(\alpha T_{t_0}) \gg 1$, the solution simplifies to

$$k \sim t^{-\alpha} \quad (13)$$

$$\varepsilon \sim t^{-1-\alpha} \quad (14)$$

Thus, for $G_0^* < 2$, so that $\alpha > 1$, and R_{T_0} small, the self-similar solution for k and ε consists of power laws with exponent depending on G_0^* , which still needs to be determined.

$$k = k_0 \left(1 + \frac{z}{\alpha T_{z0}}\right)^{-\alpha}$$

$$\alpha = (60^x - 1)^{-1}$$

$$T_{z0} = k_0 / z_0$$

$$\begin{aligned} \frac{dk}{dz} &= -\alpha k_0 \left(1 + \frac{z}{\alpha T_{z0}}\right)^{-1-\alpha} \frac{1}{\alpha T_{z0}} \\ &= -z_0 \left(1 + \frac{z}{\alpha T_{z0}}\right)^{-1-\alpha} \\ &= -z \end{aligned}$$

$$\alpha T_{z0} = \frac{k_0}{z_0 (60^x - 1)}$$

$$\frac{d}{dx}(z^x) = x z^{x-1} \frac{dz}{dx}$$

$$z = z_0 \left(1 + \frac{z}{\alpha T_{z0}}\right)^{-1-\alpha} = -(1+\alpha)$$

$$\begin{aligned} \frac{dz}{dx} &= -z_0 (1+\alpha) \left(1 + \frac{z}{\alpha T_{z0}}\right)^{-2-\alpha} \frac{1}{\alpha T_{z0}} \\ &= -z_0 (1+\alpha) \left(1 + \frac{z}{\alpha T_{z0}}\right)^{-2-\alpha} \\ &= -z_0^2 \frac{(1+\alpha)}{k_0 \alpha} \left(1 + \frac{z}{\alpha T_{z0}}\right)^{-2-\alpha} \end{aligned}$$

$$\begin{aligned} \left(1 + \frac{1}{60^x - 1}\right) 60^x - 1 \\ (60^x - 1 + 1) = 60^x \end{aligned}$$

$$z^2 = z_0^2 \left(1 + \frac{z}{\alpha T_{z0}}\right)^{-2-2\alpha}$$

$$z^2/k = \frac{z_0^2 \left(1 + \frac{z}{\alpha T_{z0}}\right)^{-2-2\alpha}}{k_0 \left(1 + \frac{z}{\alpha T_{z0}}\right)^{-\alpha}}$$

For $z/\alpha T_{z0} \gg 1$

$$= \frac{z_0^2}{k_0} \left(1 + \frac{z}{\alpha T_{z0}}\right)^{-2-\alpha}$$

i.e. z advances several

multiples of T_{z0} : $z \sim z^{-\alpha}$ and $z \sim z^{-1-\alpha}$

$$f = e^{-r^2/2\lambda_f^2}$$

$$\lambda_f^2 = 2\lambda_g^2$$

$$\frac{d}{dx}(e^u) = e^u \frac{du}{dx}$$

$$f = e^{-r^2/2\lambda_f^2} = \tilde{f}(1/\lambda_f)$$

$$G = \tilde{f}''(0)$$

$$f'' = \tilde{f}''/\lambda_f^4$$

$$\lambda_f^4 f'' = \tilde{f}''$$

$$f''(0) = \frac{12}{4\lambda_g^4} \quad \tilde{f}'' = 3 = G$$

$$f = e^{-r^2/a}$$

$$f' = -\frac{2r}{a} e^{-r^2/a}$$

$$G_0^x = \frac{7}{15} G = 7/15$$

$$a = 2\lambda_g^2$$

$$f'' = -\frac{2}{a} e^{-r^2/a} + \frac{4r^2}{a^2} e^{-r^2/a}$$

$$\alpha = (60^x - 1)^{-1} = \left(\frac{2}{3}\right)^{-1}$$

$$f''' = \frac{4r}{a^2} e^{-r^2/a} + \frac{8r^3}{a^3} e^{-r^2/a} - \frac{8r^3}{a^3} e^{-r^2/a} = 5/2$$

$$f'''' = \frac{4}{a^2} e^{-r^2/a} - \frac{8r^2}{a^2} e^{-r^2/a} + \frac{8}{a^2} e^{-r^2/a} - \frac{16r^2}{a^3} e^{-r^2/a} - \frac{24r^2}{a^3} e^{-r^2/a} + \frac{16r^4}{a^4} e^{-r^2/a}$$

EFD and theory (solution isotropic/self-similar Karman-Howarth equation using assigned value for G_0^* , as per Part 3; and other solution approaches) shows that f is Gaussian in the final period of decay:

$$f(r, t) = e^{-\frac{r^2}{2\lambda_g^2}} = \frac{\overline{u(x, t)u(x+r, t)}}{\overline{u^2}} \quad (15)$$

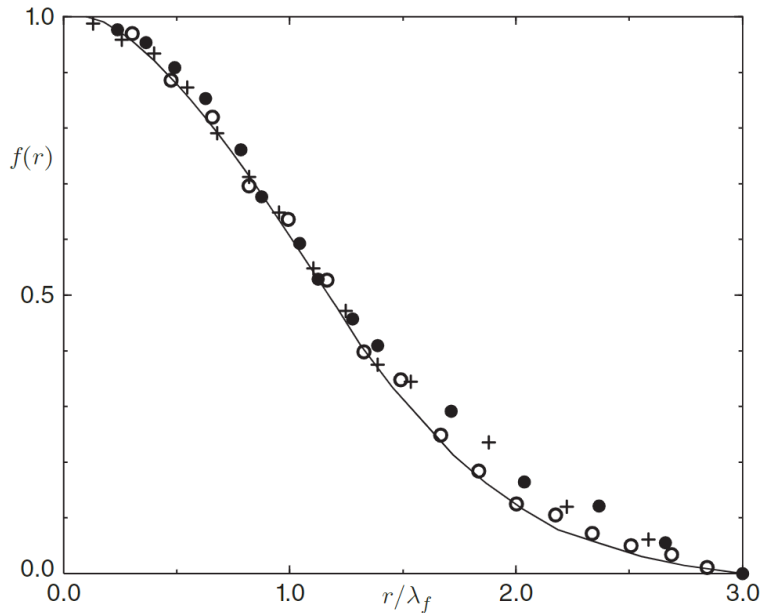


Figure 5.1 Measured and predicted $f(r/\lambda_f)$ in the final period [2]. With permission of the Royal Society.

And substituting this relation into

$$G = \tilde{f}^{IV}(0)$$

Yields

$$G = 3$$

So that

$$G_0^* = 7/5$$

$$G_0^* = \frac{7}{15}G$$

and $\alpha = 5/2$, according to Eq. (12). Using Eq. (13), k obeys a $-5/2$ decay law in the final period if the decay is self-similar. $G_0^* = 7/5$ same value used previously for $R_{T_0} < 0.1$, i.e., in the vicinity of $R_{T_\infty} = 0$.

Using $\alpha = 5/2$ and k_0 and ε_0 IC:

$$k = k_0 \left(1 + \frac{5t}{2T_{t_0}}\right)^{-5/2} \begin{array}{l} \uparrow \\ t \gg T_{t_0} \\ \approx \frac{5k_0}{2T_{t_0}} t^{-5/2} \end{array}$$

$$\varepsilon = \varepsilon_0 \left(1 + \frac{5t}{2T_{t_0}}\right)^{-7/2} \begin{array}{l} \downarrow \\ t \gg T_{t_0} \\ \approx \frac{5\varepsilon_0}{2T_{t_0}} t^{-7/2} \end{array}$$

Dissipation decays at a higher rate $t^{-7/2}$ than TKE; and balances dk/dt .

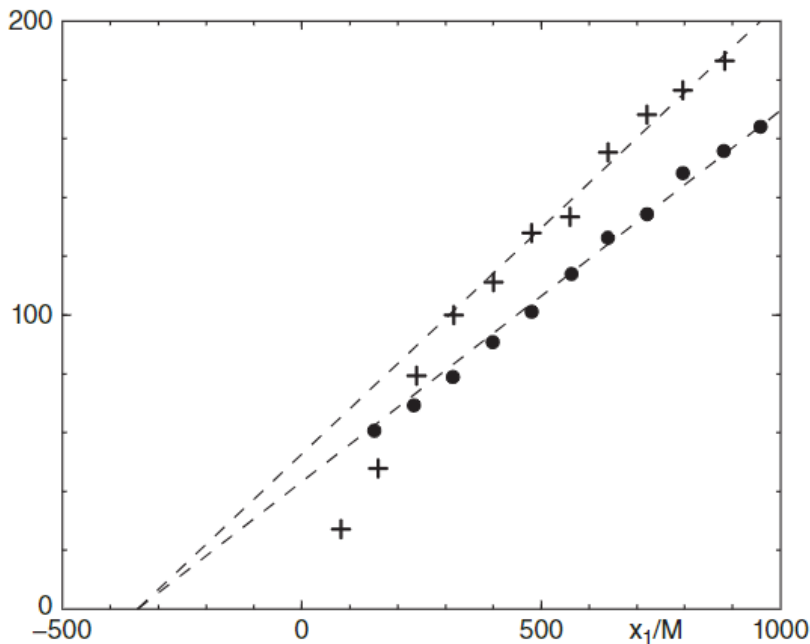


Figure 5.2 Confirmation of the $-5/2$ decay law in the final period [2]. •, $(U_m^2/\overline{u^2})^{2/5}$; +, λ_f^2 . With permission of the Royal Society.

Fig. 5.2 shows EFD for grid turbulence with mesh spacing M . Decay time $t = x_1/U_m$, where U_m represents the mean velocity and x_1 the distance along the wind tunnel. **Grid $Re = UM/\nu = 650$.**

Linear behavior of $(U_m^2/\overline{u^2})^{2/5}$ indicates that $\overline{u^2}$ satisfies a $-5/2$ decay law, and therefore, so will k for isotropic turbulence. It is concluded that the equilibrium solution associated with $R_{T_\infty}^* = 0$ when $G_0^* = 7/5$ is consistent with EFD.

As per Chapter 4 Part 3,

$$\lambda_g^2 = \frac{10\nu k}{\varepsilon}$$

$$\text{(From } \varepsilon = \frac{15\nu\overline{u^2}}{\lambda_g^2} \text{ with } k = \frac{3}{2}\overline{u^2}\text{)}$$

Substituting Eqs. (13) $k \sim t^{-\alpha}$ and (14) $\varepsilon \sim t^{-1-\alpha}$ shows that in the final period

$$\lambda^2 \sim t$$

Where λ can be either λ_g or λ_f , so that $\lambda \propto \sqrt{t}$, i.e., grows \sqrt{t} with explanation that small-scale motions vanish faster than large-scale motions, causing the scale of the surviving turbulence to increase. As the flow relaminarizes, $f(r) \rightarrow 1$ and $\lambda \rightarrow \infty$, as per Fig. 5.2, where λ_f varies linearly with x_1/M .

Also, since

$$g = f + \frac{r}{2}f'$$

The following is obtained,

$$g(r, t) = \left(1 - \frac{r^2}{2\lambda_g^2}\right) e^{-\frac{r^2}{2\lambda_g^2}}$$

Which is < 0 for $r > \sqrt{2}\lambda_g$.

For small R_T and $G_0^* < 2$, the $R_{T_\infty}^* = 0$ solution shows reasonable physics. However, this is not the case for large R_T since solutions assuming fixed-point $R_{T_\infty}^* = 0$ and $G_0^* < 2$ and large R_{T_0} display non-physical results. This is shown via solutions Eq. (4):

$$\frac{dR_T^*}{d\tau} = R_T^* (G_0^* - 2 - S_{k_0}^* \sqrt{R_T^*}) \quad (4)$$

In this case since R_{T_0} large, and $S_{k_0}^*$ cannot be neglected.

Exact solution

$$R_T^* = R_{T_0}^* \left[\frac{(G_0^* - 2) \exp((G_0^* - 2)\tau/2)}{G_0^* - 2 - S_{k_0}^* \sqrt{R_{T_0}^*} (1 - \exp((G_0^* - 2)\tau/2))} \right]^2 \quad (16)$$

When $G_0^* \neq 2$, and

$$R_T^* = R_{T_0}^* \left[\frac{1}{1 + S_{k_0}^* \sqrt{R_{T_0}^*} \tau/2} \right]^2 \quad (17)$$

when $G_0^* = 2$.

For $G_0^* < 2$ and $R_{T_0}^*$ large, if τ is large enough, Eq. (16) gives,

$$R_T^* \sim e^{(G_0^* - 2)\tau}$$

Which will tend to be small regardless of $R_{T_0}^*$, i.e., R_T^* will rapidly decrease as τ increases no matter how large $R_{T_0}^*$. And since (Chapter 5 Part 1 pg. 16),

$$\tau(t) = \ln(k(0)/k(t))$$

or

$$e^{\tau(t)} = \frac{k(0)}{k(t)} \Rightarrow k(t) = \frac{k(0)}{e^\tau}$$

i.e., $k(t) \ll k(0)$ and most energy gone.

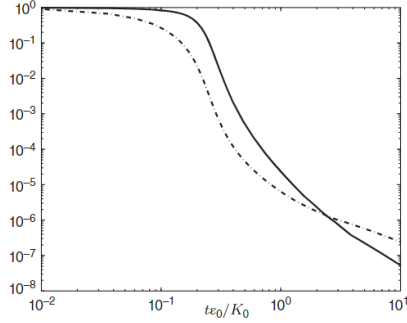


Figure 5.3 Self-similar decay corresponding to $G_0^* = 7/5$ and $R_{T_0}^* = 1000$: —, K/K_0 ; ---, R_T/R_{T_0} .

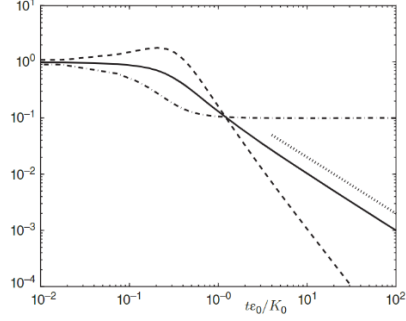


Figure 5.4 Self-similar decay corresponding to $G_0^* = 5$ and $R_{T_0}^* = 1000$: —, K/K_0 ; ---, ϵ/ϵ_0 ; ···, R_T/R_{T_0} ; ·-·-, line of slope -1.

Fig. 5.3 shows the self-similar solution for small R_T , with $R_{T_\infty}^*$ given by Eq. (6) $R_{T_\infty}^* = 0$. On the abscissa of the figure, time is scaled by initial eddy turnover $T_{t_0} = k_0/\epsilon_0$ such that when $t\epsilon_0/k_0 = 1$, one eddy turnover has occurred. During this time, k drops 5 orders of magnitude in one time unit and R_T rapidly falls to values representative of final decay.

The equilibrium solution shown next for high R_T with $R_{T_\infty}^*$ given by Eq. (7), is shown in Fig. 5.4: k drops by ~ 1 order of magnitude in one eddy turnover, while R_T approaches $R_{T_\infty}^*$. For $G_0^* = 5$, $R_{T_0}^* = 10^3$ and $S_{k_0}^* = 0.23$

$$R_{T_\infty}^* = \left(\frac{G_0^* - 2}{S_{k_0}^*} \right)^2 \sim 170$$

Drops by 1 order of magnitude, as shown in Fig. 5.4

Therefore, the drop in k obtained from the low R_T solution is unphysical.

Conclusion: for $G_0^* < 2$ and $R_{T_\infty}^* = 0$

$$\frac{dR_T^*}{d\tau} = R_T^* (G_0^* - 2 - S_{k_0}^* \sqrt{R_T^*})$$

cannot apply to the initial high Re stage of isotropic decay. In contrast to the -5/2 decay law predicted by self-similar theory and fixed-point solution, Saffman approach leads to -6/5 decay law. Both laws justified EFD depending on choice of virtual origin. Rise in λ during the final stage of decay makes it difficult to resolve this issue.

High Re Equilibrium: fixed point solution

For $G_0^* > 2$ and $R_{T_\infty}^* \neq 0$, R_{T_0} approaches $R_{T_\infty}^*$ from above or below depending on whether R_{T_0} is $<$ or $>$ $R_{T_\infty}^*$.

$$\frac{d\varepsilon}{dt} = S_{k_0}^* R_T^{1/2} \frac{\varepsilon^2}{k} - G_0^* \frac{\varepsilon^2}{k} \quad (18) = (3b)$$

But

$$S_{k_0}^* = \frac{(G_0^* - 2)}{\sqrt{R_{T_\infty}^*}} \quad \boxed{R_{T_\infty}^* = \left(\frac{G_0^* - 2}{S_{k_0}^*}\right)^2} \quad (7)$$

Therefore, as R_T approaches $R_{T_\infty}^*$:

$$\frac{d\varepsilon}{dt} = \underbrace{(G_0^* - 2) \frac{\varepsilon^2}{k}}_{\substack{\text{Vortex} \\ \text{stretching}}} - \underbrace{G_0^* \frac{\varepsilon^2}{k}}_{\substack{\text{Dissipation} \\ \text{of } \varepsilon}}$$

And thus

$$\frac{d\varepsilon}{dt} = -2 \frac{\varepsilon^2}{k} \quad (19)$$

According to Eq. (7), very large $R_{T_\infty}^*$ requires large G_0^* , assuming EFD $S_{k_0}^*$ (≈ 0.3) values. $R_{T_\infty}^* = 10^4$ gives $G_0^* = 25$, which gives near balance between vortex stretching and dissipation of ε terms in the $\frac{d\varepsilon}{dt}$ equation which is an important result \rightarrow if $G_0^* \gg 2 \Rightarrow G_0^* - 2 \approx G_0^*$; thus, vortex stretching \sim dissipation with slight edge towards dissipation resulting in Eq. (19) with net dissipation coefficient -2, i.e., for high Re equilibrium (fixed-point) decay has nearly equal contributions vortex stretching and dissipation such that **dissipation rate (per unit $\frac{\varepsilon^2}{k}$) assumes universal value, which is independent of G_0^* .** Note that vortex stretching only implicitly included in $\frac{d\varepsilon}{dt}$ equation.

Similar analysis as for $R_{T_\infty}^* = 0$ of Eq. (10) and (11), for solutions Eq. (10) and (19) for k and ε are asymptotic power laws, where comparing with Eqs. (11) and (19), shows that:

$$\alpha = \frac{1}{2-1} = 1$$

$$k \sim t^{-1} \quad \varepsilon \sim t^{-2}$$

where dissipation decays higher rate than TKE and the decay rate does not depend on G_0^* , differently from the $R_{T_\infty} = 0$ case.

$$k = k_0 \left(1 + \frac{t}{T_{t_0}}\right)^{-1} \approx \frac{k_0}{T_{t_0}} t^{-1}$$

$$\varepsilon = \varepsilon_0 \left(1 + \frac{t}{T_{t_0}}\right)^{-2} \approx \frac{\varepsilon_0}{T_{t_0}^2} t^{-2}$$

After t advances several multiples of T_{t_0} , such that $t/(\alpha T_{t_0}) \gg 1$, the solution simplifies

Since final solution independent $R_{T_0} \neq R_{T_\infty}$, a transient period exists prior to reaching R_{T_∞} wherein the coefficient in Eq. (3b) $S_{k_0} \sqrt{R_T} \rightarrow S_{k_0} \sqrt{R_{T_0}} \rightarrow G_0^* - 2$. The equations show that $R_{T_0} \rightarrow R_{T_\infty}$ in very short time, i.e., just a few eddy turnover times.

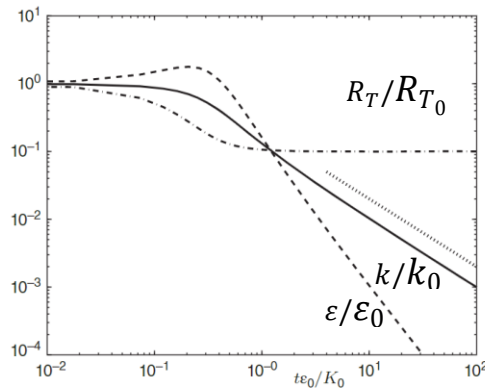
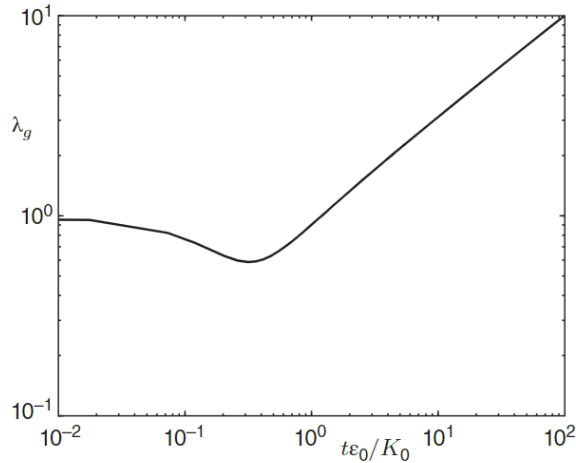


Figure 5.4 Self-similar decay corresponding to $G_0^* = 5$ and $R_{T_0}^* = 1000$: —, k/k_0 ; ---, $\varepsilon/\varepsilon_0$; ···, R_T/R_{T_0} ; ····, line of slope -1 .

Fig. 5.4 shows k , ε and R_T for $G_0^* = 5$ and $R_{T_0} = 1000$ with $S_{k_0}^* = 0.3$. In contrast to the low G_0^* solution, large R_{T_0} solution shows $k \rightarrow t^{-1}$ quickly. R_T shows initial drop and then converges to value predicted by Eq. (7). While R_T is falling, $k \sim \text{constant}$ and ε is increasing.

Figure 5.5 λ_g in isotropic decay corresponding to the conditions in Fig. 5.4.



$$\lambda_g = \sqrt{\frac{10\nu k}{\varepsilon}}$$

λ_g initially decreases, then increases due to insufficient IC energy in the dissipation range scales at the outset of the simulation.

Solution shows initial stage where energy from vortex stretching decreases λ_g and increases ε , after which stretching \sim dissipation and energy decays as per t^{-1} .

$$\lambda_g^2 = \frac{10\nu k}{\varepsilon} = \frac{10\nu}{\frac{\varepsilon_0}{T_{t_0}} t^{-2}} \frac{k_0}{T_{t_0}} t^{-1} = \frac{10\nu k_0}{\varepsilon_0} t$$

$$\lambda_g = \sqrt{\frac{10\nu k_0}{\varepsilon_0} t}$$

If $\frac{k_0}{\varepsilon_0} = \frac{2}{5} \rightarrow \lambda_g = \sqrt{4\nu t}$ recovers form from Hinze p.210. Note **Final Period of Isotropic Decay** gives same result.

Eventually, high Re solution no longer reasonable as self-similarity is lost such that G_0^* must decrease to $R_{T_\infty}^* = 0$ solution, i.e., $G_0^* = 7/5$.

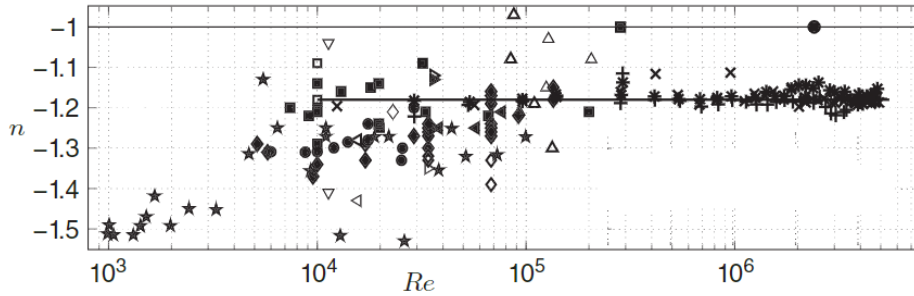


Figure 5.6 Measured power law exponents in decaying homogeneous turbulence from numerous experiments [9]. Filled symbols represent traditional turbulence behind a grid of bars. Open symbols are other turbulence sources. The symbols with \times , $*$, and $+$ are from three different probes used in decaying turbulence behind a grid of bars for which the Reynolds number was changed only by altering the viscosity of the working fluid. Used by permission of AIP.

Many EFD wide range Re , $1000 \leq R_M \leq 5 \times 10^6$, where $R_M = MU/\nu$. Average decay rate is -1.18 ± 0.02 , which suggests $k \sim t^{-6/5}$ decay law.

A small subset of the data supports the t^{-1} decay at high Re . Many complications in determining decay rate from EFD, such as IC and shift between decay laws for large and small Re .

Implications for Turbulence Modeling

Isotropic turbulence theory used for modeling ε equation as used for general flows. The two main results developed previously consist of the isotropic formulas:

$$P_\varepsilon^4 = S_k^* R_T^{\frac{1}{2}} \frac{\varepsilon^2}{k}$$

And

$$Y_\varepsilon = G^* \frac{\varepsilon^2}{k}$$

Part 1 Eq. (1) and (2a,b)

$$\frac{dk}{dt} = -\varepsilon$$

$$\begin{aligned} \frac{d\varepsilon}{dt} &= P_\varepsilon^4 - Y_\varepsilon = \nu P_\zeta^4 - \nu Y_\zeta \\ &= \left(S_k^* R_T^{\frac{1}{2}} - G^* \right) \frac{\varepsilon^2}{k} \end{aligned}$$

For general applications, it is assumed that,

$$S_k^* R_T^{\frac{1}{2}} - G^* = -C_{\varepsilon 2} \quad (20)$$

Where $C_{\varepsilon 2}$ is a constant. This leads to the model,

$$P_\varepsilon^4 - Y_\varepsilon = \left(S_k^* R_T^{\frac{1}{2}} - G^* \right) \frac{\varepsilon^2}{k} = -C_{\varepsilon 2} \frac{\varepsilon^2}{k}$$

Compare high Re equilibrium solution

$$\frac{d\varepsilon}{dt} = -2 \frac{\varepsilon^2}{k} \quad (19)$$

$$R_{T_\infty}^* = \left(\frac{G_0^* - 2}{S_{k_0}^*} \right)^2 \quad (7)$$

Which yields an equation identical to Eq. (19), i.e., high Re equilibrium, except that the constant on the RHS is $-C_{\varepsilon 2}$.

In isotropic turbulence, as per Chapter 5 Part 1, $Y_\varepsilon = \nu Y_\zeta$ which can be shown using the identity (Chapter 5 Part 1 Eq. (2a) and (2b) for LHS and first equality),

$$\overline{\left(\frac{\partial^2 u_i}{\partial x_j \partial x_l} \right)^2} = 2\nu^2 \overline{\frac{\partial \omega_i}{\partial x_k} \frac{\partial \omega_i}{\partial x_k}} = \overline{\left(\frac{\partial \omega_i}{\partial x_j} \right)^2} = Y_\varepsilon = \nu Y_\zeta = G^* \frac{\varepsilon^2}{k}$$

Second equality = Palenstrophy (Part 1), i.e., Y_ε and νY_ζ , which are dissipation of ε and ζ , respectively, involve process of decay of Enstrophy $= \frac{\omega^2}{2} = \frac{\omega \cdot \omega}{2}$.

Next, using $\varepsilon = \nu\zeta$, it follows that,

$$G^* \sim \frac{Y_\zeta/\zeta}{\varepsilon/k} = \frac{\text{Fractional rate of change of } \zeta}{\text{Fractional rate of change of energy}}$$

$$G^* = \frac{k}{\varepsilon^2} Y_\varepsilon = \frac{k}{\varepsilon^2} \nu Y_\zeta = \frac{k\nu Y_\zeta}{\varepsilon\nu\zeta} = \frac{Y_\zeta/\zeta}{\varepsilon/k}$$

That is ratio is inverse of time scales and since ζ dissipation influenced mostly by small-scale phenomena \rightarrow numerator scales with Kolmogorov $t_d^{-1} = (\nu/\varepsilon)^{-1/2}$ (Chapter 4 Part 3 pg. 1) and substituting this into the previous equation gives,

$$G^* = \frac{(\nu/\varepsilon)^{-1/2}}{\varepsilon/k}$$

$R_T = \frac{k^2}{\nu\varepsilon}$

$$G^* \sim \sqrt{R_T}$$

for large Re, which is consistent with and justifies/explains Eq. (20), which cancels the vortex stretching term. Recall again for isotropic turbulence,

$$\begin{aligned} \frac{d\varepsilon}{dt} &= S_k^* R_T^{1/2} \frac{\varepsilon^2}{k} - G^* \frac{\varepsilon^2}{k} \\ &= \left(S_k^* R_T^{1/2} - G^* \right) \frac{\varepsilon^2}{k} \\ &= \left[S_k^* R_T^{1/2} - \left(S_k^* R_T^{1/2} + C_{\varepsilon_2} \right) \right] \frac{\varepsilon^2}{k} = -C_{\varepsilon_2} \frac{\varepsilon^2}{k} \end{aligned}$$

i.e., coefficient $-C_{\varepsilon_2}$ chosen to cancel vortex stretching term, i.e., the assumption in Eq. (20) is equivalent to imposing equilibrium structure on the turbulent decay process, which imposes a decay law of the form,

$$k \sim t^{-\frac{1}{C_{\varepsilon_2}-1}}$$

i.e., C_{ε_2} sets the decay rate. e.g., for $C_{\varepsilon_2} = 11/6$, Saffman $t^{-6/5}$ law recovered.

Other values can be achieved via specification of C_{ε_2} . In all cases, without vortex stretching. If vortex stretching is included, then eventually t^{-1} decay law will develop.

Another problem is for $\nu \rightarrow 0$

$$\frac{d\varepsilon}{dt} = 0$$

i.e., ε and ζ are constant. This outcome is unphysical since it is expected that ζ should grow due to vortex stretching in the absence of dissipation.

$$\frac{d\varepsilon}{dt} = \left(S_k^* R_T^{1/2} - G^* \right) \frac{\varepsilon^2}{k}$$

For $\nu \rightarrow 0$, can be written as¹

$$\frac{d\varepsilon}{dt} = S_{k\infty}^* \zeta^{3/2} \quad (21) \quad \zeta = \varepsilon/\nu$$

Integrating Eq. (21) shows that,

$$\zeta(t) = \zeta(0) \left(1 - \frac{S_{k\infty}^* \sqrt{\zeta(0)} t}{2} \right)^{-2}$$

i.e., $\zeta \rightarrow \infty$ for $t = 2/S_{k\infty}^* \sqrt{\zeta(0)}$. This suggests vortex stretching should be explicitly included in $d\varepsilon/dt$ equation.

¹ Lesieur, M., 2008, *Turbulence in Fluids* Springer 4th Edition.

Grid turbulence (Pope 5.4.6)

A good approximation to decaying homogeneous turbulence can be achieved in wind-tunnel experiments by passing a uniform stream through a turbulence generating grid.

$$\underline{U} = U_0 \hat{i}, \quad \nabla \underline{U} = 0, \quad P = -\overline{u_i u_j} \frac{\partial \overline{U}_i}{\partial x_j} = 0$$

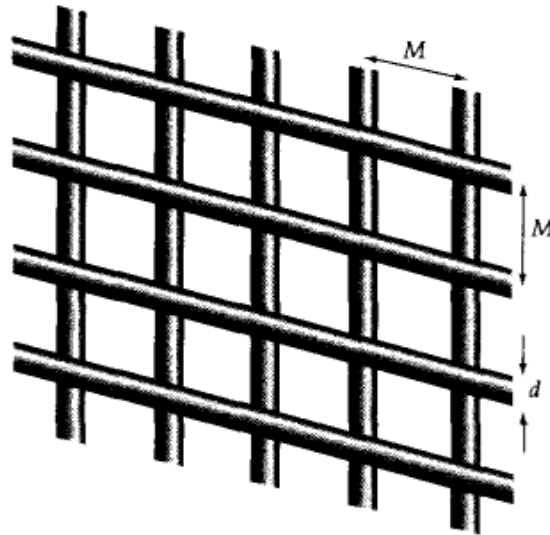


Fig. 5.32. A sketch of a turbulence-generating grid composed of bars of diameter d , with mesh spacing M .

In reference frame moving with U_0 , the turbulence is homogeneous and evolves with $t = x/U_0$.

Ideally

$$\begin{aligned} \overline{u_1^2} &= \overline{u_2^2} = \overline{u_3^2} \\ \overline{u_i u_j} &= 0 \quad i \neq j \end{aligned}$$

EFD:

$$\overline{u_2^2} = \overline{u_3^2}$$

And

$$\overline{u_i u_j} = 0 \quad i \neq j$$

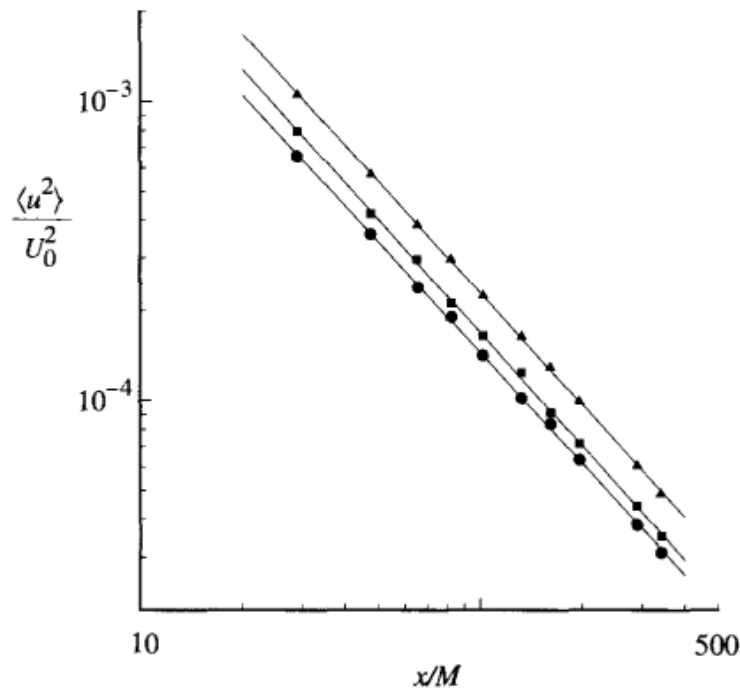


Fig. 5.33. The decay of Reynolds stresses in grid turbulence: squares, $\langle u^2 \rangle/U_0^2$; circles $\langle v^2 \rangle/U_0^2$; triangles k/U_0^2 ; lines, proportional to $(x/M)^{-1.3}$. (From Comte-Bellot and Corrsin (1966).)

$$\sqrt{\langle u_1^2 \rangle} = 10\%U_0 > \sqrt{\langle u_2^2 \rangle}$$

However, some improvements are possible.

Fig. 5.33 shows that normal stresses and k decay as power laws,

$$\frac{k}{U_0^2} = A \left(\frac{x - x_0}{M} \right)^{-n}$$

Where x_0 is the virtual origin, and $1.15 \leq n \leq 1.45$. Some suggest $n = 1.3$ and $x_0 = 0$, whereas the value of A varied widely depending on grid geometry and Re .

In moving frame

$$k(t) = k_0(t/t_0)^{-n}$$

Where $k_0 = k(0)$.

Differentiating, the following equation is obtained,

$$\frac{dk}{dt} = -\left(\frac{nk_0}{t_0}\right)\left(\frac{t}{t_0}\right)^{-(n+1)}$$

And comparing with $\frac{dk}{dt} = -\varepsilon$

$$\varepsilon(t) = \varepsilon_0 \left(\frac{t}{t_0}\right)^{-(n+1)}$$

Where $\varepsilon_0 = nk_0/t_0$.

Final period of decay: Re goes down, such that inertia \ll viscous effects. Karman-Howarth equation neglects inertia term and assuming self-similarity

$$f(r, t) = \exp(-r^2/8vt)$$

Such that $n = 5/2$.

EXERCISE

- 5.42 For grid turbulence, given the decay laws for k and ε (Eqs. (5.274) and (5.277), and taking $n = 1.3$), verify the following behaviors:

$$\begin{aligned} \tau &\equiv \frac{k}{\varepsilon} \sim t, \\ L &\equiv \frac{k^{3/2}}{\varepsilon} \sim \left(\frac{t}{t_0}\right)^{(1-n/2)} = \left(\frac{t}{t_0}\right)^{0.35}, \\ \frac{k^{1/2}L}{\nu} &\sim \left(\frac{t}{t_0}\right)^{(1-n)} = \left(\frac{t}{t_0}\right)^{-0.3}. \end{aligned}$$

(Note that the Reynolds number $k^{1/2}L/\nu$ decreases. The increase of L and τ should not be misunderstood. It is not that the turbulent motions become larger and slower. Rather, the smaller, faster motions decay more rapidly, leaving behind the larger, slower motions.)